J. Phys. B: At. Mol. Phys. 17 (1984) L771-L777. Printed in Great Britain

LETTER TO THE EDITOR

Singlet–triplet mixing in Hg 6s photoionisation via autoionising transitions

G Schönhense†, F Schäfers†, Ch Heckenkamp†, U Heinzmann† and M A Baig‡

† Fritz-Haber-Institut der Max-Planck-Gesellschaft, Faradayweg 4-6, D-1000 Berlin 33, West Germany

‡ Physikalisches Institut der Universität, D-5300 Bonn 1, West Germany

Received 20 August 1984

Abstract. New experimental photoabsorption cross section and angle-resolved photoelectron spin polarisation data for mercury are presented. For the first three autoionisation resonances above the Hg 6s threshold an analysis is performed in terms of transition amplitudes to the singlet and triplet continua. These quantities reveal that photoionisation dynamics is largely influenced by a rather complicated spectral behaviour of the triplet matrix element, including three changes of sign. Results are compared with quantum defect differences and ratios of oscillator strengths from the discrete spectrum.

Since the early work of Beutler (1933a, b) the interaction of a discrete atomic state with a continuum channel has received a great deal of attention. A detailed treatment of such autoionisation processes by configuration interaction has been given by Fano (1961). This theoretical framework was applied to a number of specific cases in atomic photoionisation, and excellent agreement between *ab initio* calculations and experiments was achieved for certain systems such as the noble gases (see, for example, Johnson *et al* 1980 and references therein). The most sophisticated theoretical models are now capable of predicting quantitatively not only the resonance behaviour of the photoionisation cross section but also features such as the photoelectron's angular distribution and spin orientation—quantities which depend very sensitively upon weak interactions, e.g. relativistic and many-electron effects.

An especially interesting system, which has been subject of a lot of experimental studies, is the autoionisation range of mercury just above the Hg 6s threshold ($h\nu =$ 10.43 eV). Up to now, no quantitative theoretical calculation for that spectral region has become available. A recent RRPA calculation for Hg showed rather good agreement with experimental data above the Hg 5d thresholds, but failed to reproduce the strong autoionisation features above 10.43 eV (Johnson *et al* 1982, 1983). It is the purpose of this Letter to present new data of the angular dependence of the photoelectron polarisation and as yet unpublished high-resolution photoabsorption results and to perform a re-evaluation of all experimental data for the first three autoionisation resonances. The analysis results in 'experimental' dipole matrix elements including their relative phase for transitions from the Hg $^1S_0$ ground state to the $^1P_1$ and $^3P_1$ continuum states of the system photoelectron + ion core (*LS* coupling scheme). The derivation is based upon measurements of the absolute and differential photoionisation cross section and three photoelectron spin-polarisation parameters. In an earlier paper

0022-3700/84/220771+07$02.50

(Schäfers *et al* 1982) we have given an analysis of the same spectral region in the framework of the *jj* coupling scheme, i.e. considering the transitions of a bound 6s electron into the continua $\varepsilon p_{1/2}$ and $\varepsilon p_{3/2}$. An advantage of the present results is that they allow a direct comparison with quantum defect differences and ratios of oscillator strengths of the corresponding $6snp\ ^1P_1$ and $^3P_1$ Rydberg series in the discrete spectrum below the threshold.

The following three autoionising transitions are studied (assignments were given by Garton and Connerade 1969):

$$\text{Hg } 5d^{10}6s^2(^1S_0) + h\nu \begin{cases} \rightarrow \begin{cases} \text{Hg } 5d^9 6s^2(^2D_{3/2})6p(^1P_1) \\ \text{Hg } 5d^9 6s^2(^2D_{3/2})6p(^3D_1) \\ \text{Hg } 5d^9 6s^2(^2D_{5/2})7p(^1P_1) \end{cases} \\ \rightarrow \text{Hg } 5d^{10}6s(^2S_{1/2})\varepsilon p(^1P_1, {}^3P_1). \end{cases} \tag{1}$$

The autoionising states belong to three different series converging to the fine-structure split d thresholds with ionic configurations $^2D_{3/2}$ (first two resonances) and $^2D_{5/2}$ (third resonance).

Owing to parity and angular momentum conservation, the photoelectron can only have the single orbital angular momentum $l = 1$ and $J = 1$ after the dipole transition. The photoelectron's spin and the net spin of the ion core can, however, either remain coupled into a singlet through the ionisation process, or change to a triplet as a consequence of spin–orbit forces. We describe the transitions to the singlet and triplet continua by the amplitudes D_S and D_T (reduced real matrix elements), respectively, and the corresponding relative phase $\delta_S - \delta_T$. In the framework of the angular momentum transfer formalism (Dill and Fano 1972, Dill 1973) the transition to the singlet continuum is the parity favoured one (angular momentum transfer $j_t = 0$), whereas the spin–flip transition to the triplet continuum is parity unfavoured ($j_t = 1$).

The set of existing experimental data for process (1) consists of:

(i) the photoionisation cross section Q (Beutler 1933a, b, Brehm 1966, scaled by Berkowitz 1979);

(ii) the photoelectron angular distribution, characterised by the asymmetry parameter β (Brehm and Höfler 1978)

$$I(\theta) \propto 1 - \tfrac{1}{2}\beta P_2(\cos\theta) \qquad (P_2(\cos\theta) = \tfrac{3}{2}\cos^2\theta - \tfrac{1}{2}) \tag{2}$$

(iii) the photoelectron polarisation component normal to the reaction plane, yielding the spin parameter ξ (Schäfers *et al* 1982)

$$P_\perp(\theta) = \frac{\xi \sin 2\theta}{1 - \tfrac{1}{2}\beta P_2(\cos\theta)} \tag{3}$$

(iv) the spin polarisation A (parallel to the photon spin) of the angle-integrated photoelectron flux (Schäfers *et al* 1982);

(v) the spin parameter α (this work), deduced from the angular dependence of the spin-polarisation transfer

$$A(\theta) = \frac{A - \alpha P_2(\cos\theta)}{1 - \tfrac{1}{2}\beta P_2(\cos\theta)}. \tag{4}$$

The spectral dependence of α, shown in figure 1, has been measured using circularly polarised synchrotron radiation from the storage ring BESSY (Berlin). Details of the experimental method are described by Heckenkamp *et al* (1984).

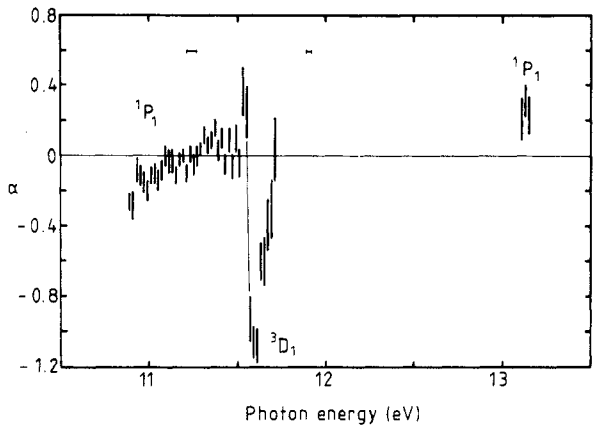

Figure 1. Autoionisation resonance structure in the asymmetry parameter α of the spin-polarisation transfer. The bandwidth of the VUV radiation was set to 60 meV in the first resonance (below $h\nu = 11.5$ eV) and to 30 meV in the second and third resonance by use of second-order radiation.

In terms of the transition amplitudes and phases, the dynamical parameters read (Lee 1974, Klar 1980, Huang and Starace 1980)†:

$$Q = \tfrac{4}{3}\pi^2 \alpha a_0^2 \omega (D_S^2 + D_T^2) \tag{5}$$

$$\beta = \frac{2D_S^2 - D_T^2}{D_S^2 + D_T^2} \qquad \xi = \frac{3\sqrt{2} D_S D_T \sin(\delta_S - \delta_T)}{4(D_S^2 + D_T^2)} \tag{6, 7}$$

$$A = \frac{D_T^2 - 2\sqrt{2} D_S D_T \cos(\delta_S - \delta_T)}{2(D_S^2 + D_T^2)} \qquad \alpha = \frac{-D_T^2 - \sqrt{2} D_S D_T \cos(\delta_S - \delta_T)}{D_S^2 + D_T^2}. \tag{8, 9}$$

It is remarkable that in this *LS* basis, the asymmetry parameter β depends incoherently upon the matrix elements, with the consequence that the parity-favoured transition yields $\beta = 2$ and the parity-unfavoured one $\beta = -1$. The spin parameter ξ is given by a single interference term containing the sine of the phaseshift difference, i.e. it changes sign whenever one of the amplitudes goes through zero or when $\delta_S - \delta_T$ goes through $n\pi$ $(n = 0, 1, 2, \ldots)$. If only the parity-favoured transition occurred, the three spin parameters would vanish, because all terms in the numerators contain D_T.

The analysis proceeded as follows: The data of Q and β yielded the squares of the amplitudes, then A gave the value of $|\cos(\delta_S - \delta_T)|$, and finally ξ and α were used to determine the signs of the amplitudes and of the phaseshift difference. Our results are shown in figure 2; the error bars contain the uncertainties of all experimental quantities involved. The singlet and triplet amplitudes show quite different behaviour: the parity-favoured D_S follows the shape of the cross section curve and is always different from zero, whereas the unfavoured D_T exhibits three changes of sign. In the

† It must be pointed out that the nomenclatures used by different authors are not identical.

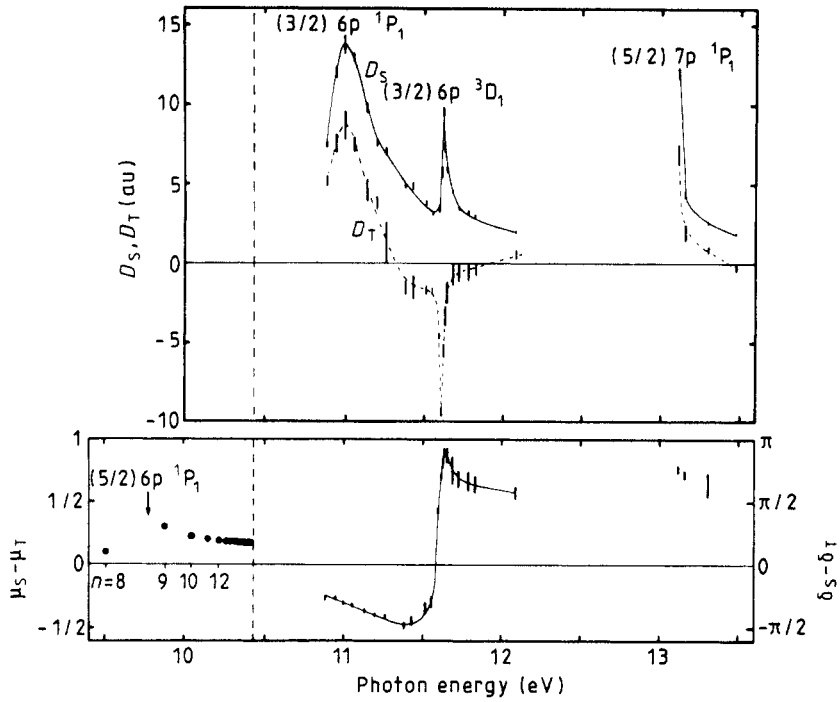

Figure 2. Singlet and triplet amplitudes (top) and corresponding phaseshift difference (bottom) plotted against photon energy. Vertical broken line, Hg 6s threshold; points below threshold, quantum defect difference $\mu_S - \mu_T$. Curves through the error bars are to guide the eye.

two $^1P_1$ resonances, both amplitudes have the same sign and almost the same shape, with D_S being roughly twice as large as D_T. The corresponding phase difference (lower part of the figure) varies only weakly across these resonances. For the $^3D_1$ resonance, however, we find completely different conditions. Here the triplet amplitude is negative† and reaches about the same absolute values as D_S does. The phaseshift difference between the singlet and triplet partial continuum waves undergoes a sudden change in this region, showing a spectral shape which is typical for the variation of a relative phase across a resonance.

The quantity $\delta_S - \delta_T$ is the difference in the phaseshifts experienced by the outgoing photoelectron with its spin either antiparallel or parallel to the spin of the remaining ion core (i.e. the spin of the second valence electron). Since in both cases $l = 1$ (εp) this phaseshift difference contains no Coulombic part and is thus strongly related to the quantum defect difference $\mu_S - \mu_T$ of the corresponding Rydberg series 6snp $^1P_1^\circ$ and 6snp $^3P_1^\circ$ converging to the first threshold. In complete accordance with the quantum mechanical meaning of $\delta_S - \delta_T$, the quantity $\mu_S - \mu_T$ is also a measure of the difference in the potential of the Rydberg atom when the spins of the outer and inner valence electron are coupled either to a singlet or to a triplet. In application of quantum defect theory (QDT), the difference $\delta_S - \delta_T$ in the ionisation continuum can be directly

† If D_T is assumed to be positive definite, the change of sign would be equivalent to a sudden jump by π of the corresponding phase δ_T.

compared with the quantity $\pi(\mu_S - \mu_T)$ in the discrete part of the spectrum. The lower part of figure 2 shows the experimental values of the quantum defect difference below threshold (data from figure 3, this work and Baig 1983). Although no data exist for the region between threshold and $h\nu = 10.9$ eV, the figure strongly suggests that there is a smooth variation of the curve across this gap, i.e. that the low-energy extrapolation of $\delta_S - \delta_T$ fits very well to the threshold value of $\pi(\mu_S - \mu_T)$.

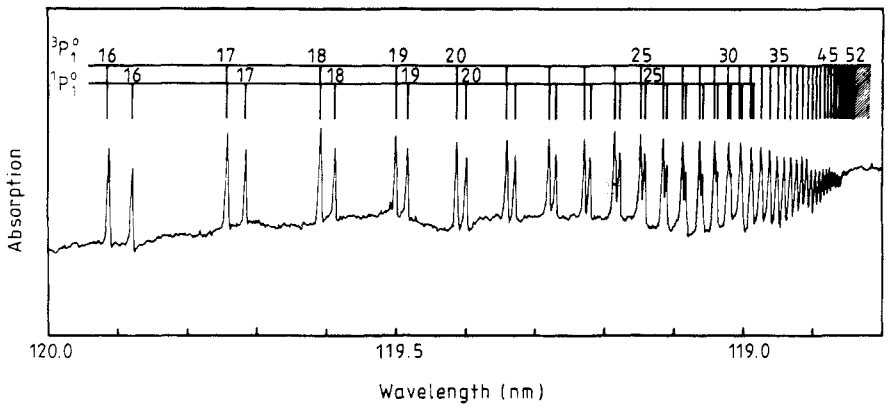

Figure 3. Densitometer trace of the photoabsorption spectrum of mercury vapour in the wavelength region from 120 nm to the first threshold at 118.787 nm. The spectrum was recorded in the first order of a 3 m spectrograph equipped with a 6000 lines/mm grating and a 10 μm slit width.

It is interesting to note that there is a perturbing level originating from the $5d^96s^2(^2D_{5/2})6p(^1P_1)$ configuration at $h\nu = 9.77$ eV (arrow in figure 2). Due to interchannel interaction between discrete configurations, the quantum-defect difference of the $6snp\ ^1P_1$, $^3P_1$ series (closed channels) is markedly affected by this perturber between $n = 8$ and 9 (for details, see Baig 1983). Analogously, the autoionising configurations above threshold act as perturbers of the open $6s\varepsilon p\ ^1P_1$, $^3P_1$ ionisation channels.

Up to now it is not possible to perform a similar comparison for the amplitudes D_S and D_T, because no absolute measurements of oscillator strengths in the discrete spectrum are available for these series. However, the high-resolution photoabsorption spectrum shown in figure 3 allows the ratios of the required oscillator strengths to be extracted. The spectrum has been recorded with the 3 m NI spectrograph at the synchrotron in Bonn using the set up described by Connerade *et al* (1980). The spectrum of the lower members of these series has been published recently (Baig 1983); the present spectrum was taken at a slightly increased resolution and at a lower vapour density. The densitometer trace has not been corrected with respect to the transmission function of the spectrograph and the sensitivity of the photographic plate. Therefore the determination of intensity ratios between adjacent lines of the principal and intercombination series may contain a systematic error. Due to the small level splitting of less than 0.04 nm above $n = 16$, however, we expect the influence of the varying transmission function and sensitivity to be negligibly small for higher n values.

The intensity ratio I_T/I_S of the absorption lines can be directly compared with D_T^2/D_S^2 taking into account the relation $I \propto D^2/n^{*3}$ (n^*, effective quantum number). Figure 4 shows the resulting ratios above and below threshold. Around 11.6 eV the

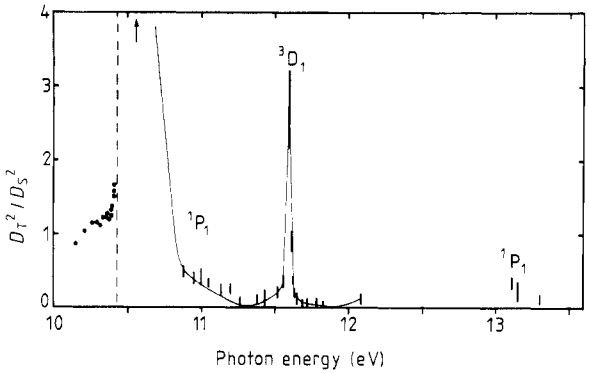

Figure 4. Ratios of the squared dipole amplitudes to the singlet and triplet continua (above threshold) and to the corresponding singlet and triplet Rydberg states (below threshold) in comparison.

triplet–singlet composition of the εp continuum is dominated by the narrow peak of the $^3D_1$ resonance. In this resonance D_T^2 exceeds D_S^2 by about a factor of 2.7 although the absolute values of D_S and D_T are nearly the same in the second resonance (cf figure 2). The reason is that D_T reaches its extremum at a significantly lower photon energy than D_S does. This narrow peak in the triplet–singlet mixing ratio is responsible for the narrow, deep minimum of $\beta = -0.17 \pm 0.12$ (Brehm and Höfler 1978). In the low-energy wing (below 10.8 eV) of the first resonance one observes again a steeply increasing ratio. From a change of sign of the spin transfer A at 10.6 eV (Schäfers *et al* 1982) we estimate a ratio of $D_T^2/D_S^2 = 8 \pm 2$ at that photon energy (arrow in figure 4) with still increasing tendency towards the threshold. This happens in a region of small cross section and is a consequence of a deep minimum (perhaps even a zero) of the singlet amplitude in the red wing of the first autoionising level. Figure 2 indicated already that in this wing D_S drops more rapidly than D_T does. In the maximum of the resonance (at 11 eV) the ratio is only 0.4, demonstrating its singlet character. The minimum of the singlet amplitude connected with the first $^1P_1$ autoionisation resonance shows up even in the discrete spectrum below threshold. According to the Fano parameterisation of this resonance performed by Brehm (1966) the resonance minimum is located in the discrete spectrum (at 124.8 nm). Figure 3 shows that with increasing energy the $^1P_1$ transitions lose oscillator strength as compared with the $^3P_1$ transitions (see also Baig 1983).

From the results of figures 2 and 4 it is evident that the $^3D_1$ level and the two $^1P_1$ levels reflect their different characters in the dynamics of the subsequent decay through autoionisation. However, we must keep in mind that the classification of these states in *LS* coupling is quite common but only an approximate labelling. Applying intermediate coupling theory with configuration interaction, Martin *et al* (1972a, b) have derived that the excited level at 11.6 eV is composed of 63.3% $^3D_1$ and 29.5% $^3P_1$, the total singlet contribution being less than 7%. On the other hand, the first resonance has 62.3% $^1P_1$, 10.3% $^3P_1$ and 24% $^3D_1$ character and the third one has 58.2% $^1P_1$, 32.1% $^3P_1$ and 9.7% $^3D_1$ character. These calculated compositions of the autoionising levels are in qualitative accordance with our results from photoelectron dynamics. The high ratio $D_T^2/D_S^2 \simeq 2.7$ near the maximum of the second ($^3D_1$) resonance means that this autoionising level decays at least at 73% into the triplet continuum. Near the maximum

of the first and third resonance ($^1P_1$) the ratio is about 0.4, i.e. these resonances decay at about 71% into the singlet continuum.

In conclusion, we have obtained the single–triplet composition (including the relative phase) of the εp ionisation continuum of Hg $6s^2$ in the spectral region just above threshold, characterised by strong autoionisation features. The analysis was based upon dynamical photoionisation parameters, which describe the differential cross section and the photoelectron spin polarisation. In the case that ionisation proceeds through an autoionising level in which the spins are coupled to a triplet, this triplet character shows up clearly in properties of the emitted photoelectrons. It is visible most pronounced in the high partial cross section ratio D_T^2/D_S^2 close to the resonance maximum and in the rapid variation of the phaseshift difference $\delta_S - \delta_T$. In the two resonances being predominantly of singlet nature the excitation of the triplet continuum is considerably lower and the phaseshift difference varies only weakly as far as experimental data exist. A strong increase of D_T^2/D_S^2 in the low-energy minimum of the first resonance gives experimental evidence of a deep minimum in the singlet amplitude just above threshold.

Although at present no complete multichannel QDT analysis is feasible for mercury, due to the lack of absolute measurements of oscillator strengths in the discrete spectrum, it was possible to compare the data obtained above threshold with quantum defect differences and ratios of oscillator strengths of the $6sn\mathrm{p}\ ^1P_1$ and $^3P_1$ Rydberg series extracted from high-resolution photoabsorption spectroscopy. Both quantities show the same tendency above and below threshold. In particular, the low-energy extrapolation of the phaseshift difference measured in the continuum fits well to the threshold value of the quantum defect difference.

Our thanks are due to the BESSY staff for useful cooperation. Support by the BMFT is gratefully acknowledged.

References

Baig M A 1983 *J. Phys. B: At. Mol. Phys.* **16** 1511
Berkowitz J 1979 *Photoabsorption, Photoionisation and Photoelectron Spectroscopy* (New York: Academic)
Beutler H 1933a *Z. Phys.* **84** 289
—— 1933b *Z. Phys.* **86** 710
Brehm B 1966 *Z. Naturf.* **21a** 196
Brehm B and Höfler K 1978 *Phys. Lett.* **68A** 437
Connerade J P, Baig M A, McGlynn S P and Garton W R S 1980 *J. Phys. B: At. Mol. Phys.* **13** L705
Dill D 1973 *Phys. Rev.* A **7** 1976
Dill D and Fano U 1972 *Phys. Rev. Lett.* **29** 1203
Fano U 1961 *Phys. Rev.* **124** 1866
Garton W R S and Connerade J P 1969 *Astrophys. J.* **155** 667
Heckenkamp Ch, Schäfers F, Schönhense G and Heinzmann U 1984 *Phys. Rev. Lett.* **52** 421
Huang K N and Starace A F 1980 *Phys. Rev.* A **21** 697
Johnson W R, Cheng K T, Huang K N and Le Dourneuf M 1980 *Phys. Rev.* A **22** 318
Johnson W R, Radojevic V, Deshmukh V P and Cheng K T 1982 *Phys. Rev.* A **25** 337
—— 1983 private communication
Klar H 1980 *J. Phys. B: At. Mol. Phys.* **13** 3117
Lee C M 1974 *Phys. Rev.* A **10** 1598
Martin W C, Sugar J and Tech J L 1972a *Phys. Rev.* A **6** 2022
—— 1972b *J. Opt. Soc. Am.* **62** 1488
Schäfers F, Schönhense G and Heinzmann U 1982 *Z. Phys.* A **304** 41